JOURNAL DE PHYSIQUE
Colloque C5, supplément au n°10, Tome 42, octobre 1981 *page* C5-433

DYNAMIC INTERNAL FRICTION IN Al

E. Bonetti*, L. Castellani*, E. Evangelista* and P. Gondi* *

* *Istituto di Fisica "A. Righi" Università di Bologna, Unità GNSM del CNR, Via Irnerio 46, 40126 Bologna, Italy.*

* *Istituto di Metallurgia Università di Roma, Via Eudossiana 18, Roma, Italy.*

Abstract.- Dynamic modulus and internal friction measurements have been carried out on Al samples directly during creep deformation. The measurements have been accompanied by observations in transmission electron microscopy. Creep curves, dynamic modulus and TEM data have been utilized for analyses with the $\phi(\ell)$ functions giving the distribution of dislocation segments both mobile and non-mobile.

1. Introduction.- The behaviour of metals during deformation, as in creep, is conditioned by the evolution of the distribution function $\phi(\ell)$ of free dislocation segments. Interpretations in this field had thus to refer more or less specifically to this subject: in particular reference can be made to the papers of Gasca Neri-Nix /1/ and of Lagneborg et al./2/ where the matter is treated in detail.

Observations giving information on $\phi(\ell)$ have been carried out by H.V. transmission electron microscopy /3/.

Information may also be obtained by dynamic modulus and Q^{-1} measurements made directly during deformation: in a previous paper /4/ we considered it with particular reference to the average dislocation segment lengths probably at the origin of the Q^{-1} peak K_1 /5,6/: here those considerations are extended to seek for indications on the nature of the $\phi(\ell)$ functions as well as on other parameters such as effective frequency in the thermal overcoming processes involving dislocations and dislocation segments contributing to modulus relaxation.

2. Experimental.- Observations were made on Al 99.99% with the following analysis:

Fe	Si	Cu	Zn	Mg	
0.0003	0.0017	0.0015	0.0002	0.0008	wt%

The specimens were rectangular with section 0.1x0.2 cm^2: Their length ranged between 10 and 20 cm. After rolling and cutting the specimens were submitted to heating

treatments at 640°C for 10 hrs leading to grain sizes ≃ 0.1 cm.

An inverted torsion pendulum, as used by other authors during deformation /7,8/ served for Q^{-1} and dynamic modulus measurements. Amplitudes were of the order of 10^{-5}. No amplitude dependence was noticed. Errors relating to Q^{-1} and M_d data are ≃ 1%.

In this paper reference is made to creep tests carried out at 150°C with loads 1.3 Kg/mm^2. For TEM observations specimens were thinned by electrolytic polishing.

3. Results.- As mentioned, results concern specimens of Al deformed by creep at 150°C. Creep curve and corresponding dynamic modulus and internal friction behaviour during deformation are given in fig. 1

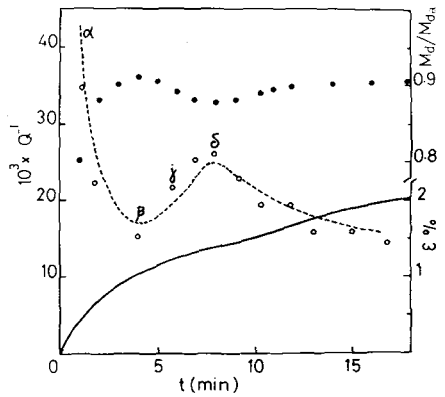

Fig. 1: Internal friction(o), dynamic modulus(●) and elongation(—) vs. time during creep: temperature 150°C, load 1.3 Kg/mm^2, frequency ≃ 6 Hz. Dashed line diagram represents the $(Q_b^{-1} + Q_M^{-1})$ behaviour calculated from relation (4) (see text).

The dynamic moduli are expressed by the ratios M_d/M_{ua}, M_{ua} being the modulus before deformation at room temperature. The concordance between the trends of M_d and Q^{-1} may be related to changes in structure connected with damping under fully or partially relaxed conditions. The unrelaxed modulus, from which the modulus defect is obtained, does not necessarily correspond to M_{ua}. It seems thus worth taking into account as modulus defect for the discussion

$$\Delta M_d/M = (M_{ux} - M_d)/M_{ux} \qquad (1)$$

M_{ux} being taken as unknown unrelaxed modulus which can be evaluated from the Q^{-1} behaviour by considering contributions to the experimental internal friction coefficient as follows:

$$Q_{exp}^{-1} = Q_d^{-1} + Q_M^{-1} + Q_b^{-1} \qquad (2)$$

Q_b^{-1} is the background damping which will be considered constant. Q_d^{-1} is the damping directly connected with viscous deformation for which the following relation is considered valid /9/:

$$Q_d^{-1} = C\dot{\varepsilon} \quad \text{with } C = 0.1\ VG/kT2\pi\nu \qquad (3)$$

V = activation volume, G = shear modulus, ν = vibration frequency.

Q_M^{-1} is the damping connected with relaxed structures, proportional to $\Delta M_d/M$ through

a coefficient μ corresponding to $\omega\tau$ for S.L.S.; μ is < or > 1 before ($M_d \rightarrow M_u$) and after ($M_d \rightarrow M_r$) Q^{-1} peak, with τ relaxation time. Thus

$$Q^{-1}_{exp} = Q^{-1}_d + Q^{-1}_M + Q^{-1}_b = C\dot{\varepsilon} + \mu\,(M_{ux} - M_d)/M_{ux} + Q^{-1}_b \qquad (4)$$

Taking $Q^{-1}_b = 10^{-2}$, which corresponds to the internal friction coefficient before deformation, there results $Q^{-1}_{exp} + Q^{-1}_b \simeq \mu(M_{ux} - M_d)/M_{ux}$ for $\mu = 0.2$ and $M_{ux} = 0.95\ M_{ua}$ Within the errors the Q^{-1}_d term depending on the viscous deformation appears negligible. The dotted line diagram in fig. 1 has been drawn introducing into (4) the said Q^{-1}_b, μ, M_{ux} values for C negligibly small: corresponding values of $\Delta M_d/M$ at four deformation levels are written in table 1.

The results of TEM observations are represented by the data in table 1 and by the histograms in fig. 2; the deformation stages to which densities, histograms, etc. refer are labelled by α, β, γ, δ in fig. 1.

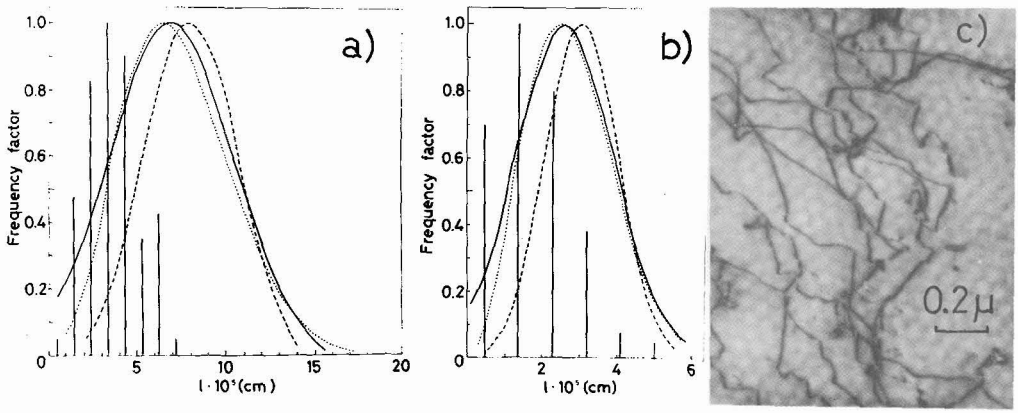

Fig. 2: a),b)-Histograms (from TEM) of dislocation free lengths (a for $\varepsilon \equiv \alpha$, b for $\varepsilon \equiv \delta$ in fig. 1). Curves calculated with functions 7a)—, 7b):···, 7c)---(see discussion). c)-TEM Micrograph showing dislocation segmentation (stage δ in fig.1)

	ε%	ρ cm^{-2}	$\bar{\ell}$ cm	$\Delta M_d/M$
α	0.5	9×10^8	5×10^{-5}	0.15
β	1.1	1×10^9	3×10^{-5}	0.04
γ	1.3	2×10^9	2×10^{-5}	0.06
δ	1.4	3×10^9	1×10^{-5}	0.07

Table 1

Dislocation density ρ, average dislocation free length $\bar{\ell}$ and modulus defect $\Delta M_d/M$ at the deformation ε.

Apart from minor corrections the dislocation densities are $(\bar{d})^{-2}$; $\bar{d}$ (± 20%) being the average dislocation distance in the projection view under the electron microscope. Average dislocation free lenghts and histograms refer to the free segments which can be resolved along each dislocation, as illustrated in fig.2c).

TEM results refer to specimens which were not submitted to deformation during the

observations: differences with respect to the pinning conditions under stress and during deformation can thus be expected whereas it will be assumed that the differences concerning the total number of dislocations per cm^2 are of minor character.

4. Discussion.- Results are discussed with reference to the dislocation segment distribution represented by the function $\phi(\ell)$. $\phi(\ell)d\ell$ gives the number of free segments per cm^3 in the range ℓ - ℓ + $d\ell$ during deformation.

Relations based on $\phi(\ell)$ which are taken into consideration are those of dislocation density ρ, modulus relaxation $\Delta M_d/M$ and deformation rate $\dot{\varepsilon}$ /2,4/.

$$\rho = \int_0^\infty \ell\phi(\ell)d\ell \qquad (5a); \qquad \xi\Delta M_d/M = \int_0^{\ell m} \eta\, \ell^3\phi(\ell)d\ell \qquad (5b)$$

$$\dot{\varepsilon} = 4\pi b\bar{\ell}^2 \int_{\alpha Gb/\sigma}^\infty \nu_d \exp -\left[\frac{H_o - b\bar{A}/\sigma_e}{kT}\right] \phi(\ell,t)d\ell \qquad (5c)$$

η = 0.1 a parameter depending on the backstresses, orientation, etc., ξ a factor that gives the amount of relaxation, $\bar{\ell} = \int_0^\infty \ell\phi(\ell)d\ell / \int_0^\infty \phi(\ell)d\ell$, ν_d and H_o vibration frequency and activation energy for the thermally activated motion of dislocations, σ_e the effective stress equal to $\sigma - \alpha Gb/\ell$, σ applied stress, α strength constant in the range 0.6÷1.27 taken =1 /10/. On account of the dependence of the activation area A on the effective stress σ_e /11/ the exponential factor is considered equivalent to

$$\exp(-H_o/kT)\ \sigma_e^{ab/kT} \qquad (6) \qquad \text{with } a = A\sigma_e$$

Besides those concerning the $\phi(\ell)$ functions, questions can be put on the vibrational frequency, on the upper limit of integration ℓm, on the relaxation factor: whether the frequency corresponds to the Debye one (ν_D) or to the one of vibration of dislocation segments ($\nu_D b/\ell$); whether the upper limit is ∞ or Gb/σ, i.e. whether mobile dislocations contribute or not to the modulus relaxation; whether $\xi \simeq 1$, i.e. nearly all dislocations are relaxed e.g. with respect to the peak observed by Esnouf et al /14/ at ∿130°C(∿1 Hz) or whether are only in part relaxed, e.g. with ξ=5 if full relaxation is related to peak K_1 /5,6/ with spread of relaxation times.

In a previous paper/4/ $\phi(\ell)$ was assumed to be Gaussian, i.e.

$$\phi(\ell) = A_1 \exp\left[-B_1(\ell - \sqrt{2/B_1})^2\right] \qquad (7a)$$

In this paper we take into consideration together with (7a) also other functions used by Lagneborg et al. /2/, i.e.

$$\phi(\ell) = A_2\ell^2\exp(-B_2\ell^2) \qquad (7b); \qquad \phi(\ell) = A_3\ell^3\exp(-B_3\ell^3) \qquad (7c)$$

Introducing these functions into the equations (5a) and (5b) the unknown parameters A_i and B_i are obtained as a function of the dislocation densities and modulus

defects experienced. The parameters so obtained have been introduced into equation (5c) and the deformation rates so calculated for two cases which appear worth of interest are represented by the broken line diagrams in fig. 4 for comparison with the experimental data.

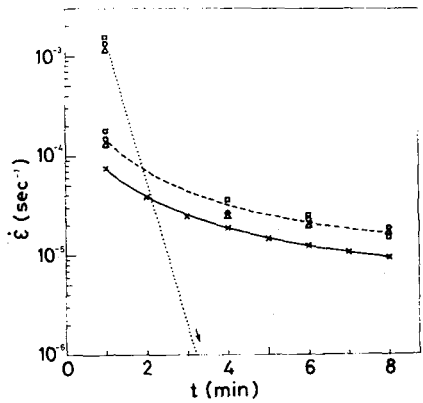

Fig. 4: Deformation rate vs. time
-x- = experimental data
△ - corresponding to function (7a)
○ - corresponding to function (7b)
□ - corresponding to function (7c)
--- H_o = 30Kcal/mole; a = $1x10^{-7}$dyne
$\nu_d^o = \nu_D(10^{13}sec^{-1})$; ξ = 5.
··· H_o = 20Kcal/mole; a = $1x10^{-7}$dyne
$^o\nu_d = \nu_D b/\ell$; ξ = 1.

The energy H_o = 20 Kcal/mole has been related to pipe diffusion along the dislocations/11,12/; H_o = 30 Kcal/mole corresponds to the energy for creep at our test temperature /11,13/.

The curves have been calculated by assuming that both mobile non-mobile dislocations can contribute to modulus relaxation: putting Gb/σ as upper limit of integration into (5b) creep rates some orders of magnitude lower result.

Values of the A_i and B_i parameters and of the average lengths $\bar{\ell}$, for the two cases considered in fig. 4 are given in table II for two deformations.

TABLE II

ε%	A_1	B_1	$\bar{\ell}_1$	A_2	B_2	$\bar{\ell}_2$	A_3	B_3	$\bar{\ell}_3$
0.5	$1.5x10^{17}$	$4.2x10^{8}$	$6.9x10^{-5}$	$1x10^{26}$	$2.4x10^{8}$	$7.3x10^{-5}$	$9.4x10^{29}$	$2x10^{12}$	$8x10^{-5}$
(H_o=30Kcal/mole)									
1.4	$3.4x10^{18}$	$2.9x10^{9}$	$2.6x10^{-5}$	$1.6x10^{28}$	$1.7x10^{9}$	$2.8x10^{-5}$	$3.9x10^{32}$	$3.6x10^{13}$	$3x10^{-5}$
0.5	$7.5x10^{17}$	$2.1x10^{9}$	$3.1x10^{-5}$	$2.6x10^{27}$	$1.2x10^{9}$	$3.3x10^{-5}$	$5.3x10^{31}$	$2.2x10^{13}$	$3.6x10^{-5}$
(H_o=20Kcal/mole)									
1.4	$1.7x10^{19}$	$1.4x10^{10}$	$1.2x10^{-5}$	$4.1x10^{29}$	$8.3x10^{9}$	$1.2x10^{-5}$	$2.2x10^{34}$	$4x10^{14}$	$1.4x10^{-5}$

For these two deformations diagrams corresponding to the functions used with the parameters given in table II and for H_o = 30Kcal/mole are drawn in fig.2, for comparison with the experimental distribution histograms which were obtained not during deformation. Calculations are limited up to deformations of 1.4% because in TEM subboundary and boundary formation is observed at larger deformations (see also /4/).

5. Conclusions.- The fact that the experimental data can be approached with H_o = 30 Kcal/mole, $\nu_d = \nu_D$, ξ = 5 is consistent with the assumption already done in previous papers /5,6/ that peak K_1,observed in correspondence of Kê peak, is connected with dislocations.

The differences with the various $\phi(\ell)$ functions used fall within the errors.

The distribution functions used are comparable to those of the dislocation segments observed in TEM after the various deformations, even if during deformation displacements towards larger average free lengths result from this analysis.

6. Acknowledgements.- The authors wish to thank Mr. R. Berti for his collaboration. The research was carried out on C.N.R. funds.

7. References.-

/1/ R. Gasca Neri and W.D.Nix, Acta Met., 22, (1974) 257.

/2/ R. Lagneborg and B. Forsen, Acta Met., 21, (1973) 781.
P. Ostrom and R. Lagneborg, J.Eng.Met. and Tech., 98, (1976) 114.

/3/ L.P. Kubin and J.L. Martin in:"Strength of Metals and Alloys", P. Haasen, V. Gerald and G. Kostorz, Editors, Pergamon Press, 1979, p. 1639.

/4/ E. Bonetti, E. Evangelista and P. Gondi, Phys.Stat.Sol.(a), 63,(1981), 645.

/5/ E. Bonetti, E. Evangelista, P. Gondi and R. Tognato, Phys.Stat.Sol.(a), 39, (1977), 661.

/6/ E. Bonetti, E.Evangelista, and P.Gondi in "Internal Friction and Ultrasonic Attenuation in Solids", C.C.Smith Editor, Pergamon Press, 1980, p.301.

/8/ P. Bourges, J.L.Gacougnolle, J.Woirgard and J.De Fouquet, Rev.Phys. Appl., 13 (1978), 1.

/7/ T.S. Kê, P.T. Yung and C.C. Chang, Sci. Sin., 1, (1957) 231.

/9/ V.S. Postnikov, Yu. M. El'Kin, S.I. Meshkov, Fiz. Tverd. Tela, 8 (1966) 3652.

/10/N.Balasubramanian and J.C.M. Li, J. Mater. Sci., 5 (1970) 434.

/11/H.Luthy, A.K.Miller and O.D.Sherby, Acta Met., 28 ,(1980) 168.

/12/T.E.Volin and R.W.Balluffi, Phys. Stat. Sol., 25 , (1968) 163.

/13/O.D.Sherby,J.L.Lytton and J.E.Dorn, Acta Met., 5, (1957) 219.

/14/C.Esnouf,M.Gabbay and G.Fantozzi, J.Physique Lett.,38, (1977) L-401.